Oil & Gas Science and Technology – Rev. IFP, Vol. 65 (2010), No. 4, pp. 565-580

DOI: 10.2516/ogst/2009071

Dossier

CO_2 Storage in the Struggle against Climate Change
Le stockage du CO_2 au service de la lutte contre le changement climatique

Evolution of the Petrophysical and Mineralogical Properties of Two Reservoir Rocks Under Thermodynamic Conditions Relevant for CO_2 Geological Storage at 3 km Depth

G. Rimmelé[1], V. Barlet-Gouédard[1*] and F. Renard[2,3]

1 Schlumberger Riboud Product Center (SRPC), Well Integrity Technologies, 1 rue Becquerel, BP 202, 92142 Clamart Cedex - France
2 University Joseph Fourier – Grenoble I, CNRS/OSUG/LGCA, Maison des Géosciences, BP 53, 38041 Grenoble - France
3 Physics of Geological Processes, University of Oslo, Oslo - Norway
e-mail: grimmele@clamart.oilfield.slb.com - vbarlet@clamart.oilfield.slb.com - francois.renard@ujf-grenoble.fr

* Corresponding author

Résumé — Évolution des propriétés physiques et minéralogiques de deux roches réservoirs dans des conditions thermodynamiques correspondant à un stockage géologique de CO_2 à 3 km de profondeur — L'injection de dioxyde de carbone (CO_2) en sous-sol pour un stockage géologique à long terme est considérée comme une solution pour contribuer à la réduction des émissions de gaz à effet de serre dans l'atmosphère. Les interactions entre le CO_2 supercritique et la roche-réservoir potentielle doivent être étudiées en détail en conditions de stockage géologique. Quarante échantillons de calcaire de Lavoux et de grès d'Adamswiller, provenant de roches réservoirs du bassin parisien, ont été expérimentalement exposés au CO_2 dans un autoclave spécialement construit pour reproduire les conditions thermodynamiques d'un réservoir de stockage de CO_2. Les deux types de roches ont été exposés pendant un mois à du CO_2 supercritique humide et à de l'eau saturée en CO_2, à 28 MPa et 90 °C, ce qui correspond à des conditions d'enfouissement de 3 km de profondeur. L'évolution de leurs propriétés minéralogiques a été suivie par des analyses par diffraction des rayons X, par spectroscopie Raman et par microscopie électronique couplée à un système de microanalyses X. Leurs propriétés physiques et microtexturales ont été estimées en mesurant, avant et après les expériences, le poids, la densité, les propriétés mécaniques, la perméabilité, la porosité globale et la présence d'éventuels gradients de porosité de chaque échantillon. Les résultats montrent que les deux roches ont préservé leurs propriétés mécaniques et minéralogiques, malgré une augmentation de la porosité et de la perméabilité. Des zones microscopiques de dissolution de la calcite observées dans le calcaire sont vraisemblablement responsables de cette augmentation de la perméabilité et de la porosité. Dans le grès, une altération de la pétro-fabrique est supposée se produire due à la réaction des minéraux argileux avec le CO_2. Tous les échantillons du calcaire de Lavoux et du grès d'Adamswiller ont montré une altération mesurable dans le CO_2 humide et dans l'eau chargée en CO_2. Ces expériences en autoclave sont effectuées en utilisant de l'eau distillée et donc simulent des conditions plus sévères que si elles étaient effectuées avec de l'eau de formation (saumure).

Abstract — Evolution of the Petrophysical and Mineralogical Properties of Two Reservoir Rocks Under Thermodynamic Conditions Relevant for CO_2 Geological Storage at 3 km Depth *— Injection of carbon dioxide (CO_2) underground, for long-term geological storage purposes, is considered as an economically viable option to reduce greenhouse gas emissions in the atmosphere. The chemical interactions between supercritical CO_2 and the potential reservoir rock need to be thoroughly investigated under thermodynamic conditions relevant for geological storage. In the present study, 40 samples of Lavoux limestone and Adamswiller sandstone, both collected from reservoir rocks in the Paris basin, were experimentally exposed to CO_2 in laboratory autoclaves specially built to simulate CO_2-storage-reservoir conditions. The two types of rock were exposed to wet supercritical CO_2 and CO_2-saturated water for one month, at 28 MPa and 90°C, corresponding to conditions for a burial depth approximating 3 km. The changes in mineralogy and microtexture of the samples were measured using X-ray diffraction analyses, Raman spectroscopy, scanning-electron microscopy, and energy-dispersion-spectroscopy microanalysis. The petrophysical properties were monitored by measuring the weight, density, mechanical properties, permeability, global porosity, and local porosity gradients through the samples. Both rocks maintained their mechanical and mineralogical properties after CO_2 exposure despite an increase of porosity and permeability. Microscopic zones of calcite dissolution observed in the limestone are more likely to be responsible for such increase. In the sandstone, an alteration of the petro-fabric is assumed to have occurred due to clay minerals reacting with CO_2. All samples of Lavoux limestone and Adamswiller sandstone showed a measurable alteration when immersed either in wet supercritical CO_2 or in CO_2-saturated water. These batch experiments were performed using distilled water and thus simulate more severe conditions than using formation water (brine).*

INTRODUCTION

Industrial injection of carbon dioxide (CO_2) underground has been experienced for several decades, for instance with enhanced oil and gas recovery operations [1-3]. For this specific application, CO_2 is injected in the reservoir for short time-scales compared to the consideration of storing supercritical CO_2 in geological reservoirs for thousands years. During the last few years, much effort has been devoted to study the behavior of well cement for CO_2 storage application [4-10]. Indeed, cement that ensures isolation between the casing and the geological formation must be durable under the severe conditions considered in such application. Furthermore, the interactions between CO_2 and the reservoir rock under geological sequestration conditions also need to be investigated. It is particularly crucial to understand the CO_2-related mineralization or dissolution processes that may be encountered deep in geological formations because these processes may control the long-term integrity of the well, the reservoir, and the cap-rocks. Three main types of geological reservoirs have sufficient capacity to store captured CO_2: depleted oil and gas reservoirs, deep saline aquifers and unminable coal beds [11].

In this study, CO_2-rock interactions under CO_2 geological storage conditions have been investigated. Two rocks were sampled from reservoir rocks in the Paris basin: the Lavoux limestone and the Adamswiller sandstone. Their evolution under pressure (28 MPa) and temperature (90°C) conditions relevant for storage in a reservoir located at 3 km depth was studied. If these conditions do not apply to a specific reservoir, they are close enough to what is found in the Earth crust, where a geotherm of 30°C/km and a fluid pressure gradient of 10 MPa/km represent average values.

This study first presents the rock materials, the equipment, and the procedure used for the CO_2 experiments, and the protocol of analysis to characterize the rocks properties evolution under these test conditions. Then, the results on the behavior of both the Lavoux limestone and the Adamswiller sandstone under reservoir conditions and CO_2-rich fluids are presented by highlighting the main petrophysical and mineralogical changes.

1 EXPERIMENTAL PROTOCOL

1.1 Rock Samples

Two porous rocks with different pore structure and mineralogical composition were used in the experiment. The Lavoux limestone, a Callovian age peloidal and bioclastic grainstone, was sampled in a quarry (Vienne, France). The rock is a quasi-pure limestone essentially composed of micritic peloids and echinoderm fragments cemented during secondary crystallization process. The mean porosity is 23%. The porosity is mainly composed by pores of 0.1-0.7 μm in size, which correspond to intra-porosity of the micritic peloids. Two others families of pores of about 1 μm and 100 μm in size correspond to the inter-grain porosity. The larger corresponds to macroscopic porosity obtained by selective leaching of peloids during possible recent meteoric diagenesis.

The Adamswiller sandstone, a Bundsandstein age sandstone, was sampled in a quarry (Bas-Rhin, France). The

rock is composed of quartz (71%), feldspar (9%) with little alteration, clay (11%), mica (5%), and traces of apatite, iron and titanium oxides. Its porosity is close to 23%, the mean grain size is 0.18 mm, and the average pore size is close to 90 μm [12]. This sandstone exhibits some lithological variations, with greenish parts intercalated by red parts. As detected by optical microscopy, the greenish areas contain more phyllosilicates (chlorite, micas) and oxides than the red parts.

1.2 Experimental Set-Up

The CO_2 setup used to perform the tests consists of a low-pressure CO_2-supply system, a high-pressure pumping system, an autoclave with its heating system *(Fig. 1)*, and a depressurization system. The autoclave has a capacity of 1.8 L and can operate up to 500ºC and about 350 bars. It is a fixed head autoclave, equipped with a magnetic drive to provide a gas-tight internal stirrer if needed. Although the body of the autoclave is made of stainless steel, all the wetted parts are either made of Hastelloy or Titanium. Adjustable titanium perforated plates are used to support the samples in the autoclave. Heating is provided by a furnace and by an additional flexible heating coil wrapped around the head of the autoclave. This ensures uniform temperature between the upper and lower parts of the autoclave, whether stirring is used or not. The entire system (valve activation, pumps, heating, depressurization phase, etc.) is monitored and controlled remotely.

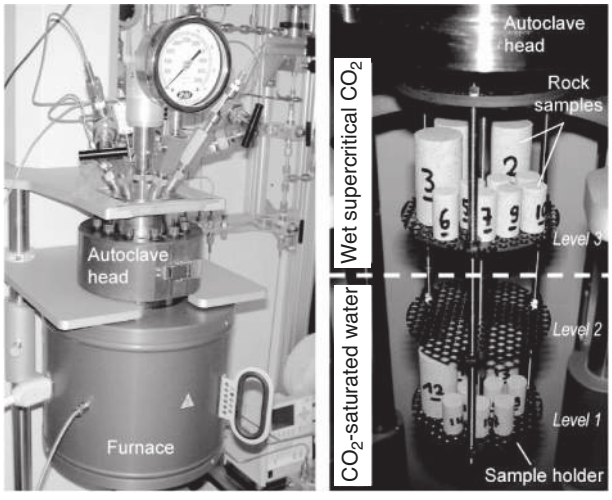

Figure 1

Picture of the autoclave enveloped by the furnace for CO_2 experiments (left) and picture of the sample holder with the configuration of the Lavoux limestone samples on the first level for immersion in CO_2-saturated water and on the third level for exposure to wet supercritical CO_2 (right).

1.3 Experimental Procedure

The experimental set-up *(see Fig. 1)* is designed to expose samples to CO_2 dissolved in water (lower part of the autoclave; Level 1) and water dissolved in pressurized CO_2, *i.e.* wet supercritical CO_2 (upper part of the autoclave; Level 3). After having loaded the samples, the required amount of water was added until the fluid has reached the middle sample holder (Level 2). When the autoclave was closed, the furnace and the heating coil were set in place. Then, the heat was slowly increased, and simultaneously the CO_2 pressure was raised regularly up to the final temperature and pressure. This step last for about 1.5 hours. During the test, temperature and pressure were monitored and maintained constant. At the end of the test period, heaters and pumping system were automatically stopped. Temperature and consequently pressure slowly dropped down. When the temperature reached 55ºC, the pressure release system was adjusted to continuously and smoothly release pressure in five hours. The overall cooling down and pressure release processes last approximately nine hours. This long depressurization phase was necessary to avoid damaging the samples.

1.4 Experimental Conditions

As it is planned to inject and store CO_2 in its supercritical state (fluid that has the viscosity of a gas, the density of a liquid and a high diffusivity), the test conditions of the experiments were 90°C and 28 MPa, corresponding to what can be measured in a geological reservoir located at depths close to 3 km. The CO_2 experiments were performed under static conditions, without applying stirring in the autoclave. We have chosen such experimental conditions because:

– they are relevant for geological storage in shallow to intermediate depth reservoirs;
– even if the fluids in a reservoir might migrate and do not stay static, we expect that they would reach some equilibrium pressure several years after injection.

These pressure and temperature conditions can be considered as a severe simulation of the CO_2 exposure in the reservoir rock. Since CO_2 is highly soluble in water, distilled water is used rather than saline solution to provide more extreme conditions [13-16]. At 90°C and 28 MPa, water is liquid while CO_2 is supercritical [17-19]. Under these conditions, the water mole fraction in the supercritical CO_2 phase is about 1.8% and the CO_2 mole fraction in water is 2.25%, which corresponds to a molarity of 1.3 $mol.kg^{-1}$ [13-16]. Furthermore, some experimental data available in the literature show that under these conditions, pH of water saturated by CO_2 is comprised between 2.8 and 3.0 [20, 21].

Both experiments with the limestone and the sandstone samples were performed during one month (720 hours). Before the experiments, the samples were stored in distilled water for a few days to ensure a complete water saturation of

the porosity. For each CO_2 test, twenty cylindrical samples were prepared from a block of rock by coring and cutting the block. The dimensions of the cylindrical samples are either 2.5-cm length × 1.25-cm diameter (14 samples) or 5.0-cm length × 2.5-cm diameter (6 samples). Ten samples were immersed in wet supercritical CO_2 and ten others in CO_2-saturated water. The volume of water introduced in the autoclave was 685 mL, so that the water level reached the middle of the sample holder *(Fig. 1)*. With such configuration, the volume ratios between the samples and water, and between the samples and supercritical CO_2, were 0.15 and 0.11, respectively.

1.5 Analysis of the Altered Samples

All the samples were measured (weight, dimensions) and photographed before and after CO_2 exposure. The density was measured by dividing each core sample weight by the weight of the displaced volume of water. Before the experiment, the samples were immersed during few days in distilled water. Then the pH of the fluid in equilibrium with the sample cores was measured. At the end of the experiment, the autoclave was open and the pH of the fluid within the vessel was measured. The altered sample cores were then removed from the experimental fluid, stored in distilled water during few days. The samples altered by wet supercritical CO_2 and those by CO_2-saturated water were stored in different boxes. The pH of water at the equilibrium with the altered sample cores was measured after few days, and was compared to the initial one.

Unconfined Compressive Strength (UCS) of the samples was measured with an MTS/*Adamel* (model 20/M) press. Mechanical properties were measured on cores presenting planar surfaces and perpendicular to the cylindrical axis. The compressive strength was measured on 2.5-cm length × 1.25-cm diameter samples with the 5 kN or 100 kN set-up. The Young's modulus and Poisson's ratio were measured on 5.0-cm length × 2.5-cm diameter samples. Measurements on at least two samples were performed for each rock. The maximal applied stress was equal to half of the UCS. Axial displacement rate was equal to 0.05 mm/min. Three consecutive load/unload cycles were performed. The Young's modulus and Poisson's coefficient were determined on the two last cycles.

Water-permeability measurements were performed by an external laboratory on the samples before and after CO_2 exposure. The water flow was measured on 5.0-cm length × 2.5-cm diameter cylinder cores, under an effective confining pressure of 2.8 MPa and a differential pressure of 3.5 MPa. For each sample, two measurements were performed to check the repeatability. These measurements are performed on one or two samples of the rock, before and after exposure. The detection limit of the measurements is in the range (1-5) $\times 10^{-18}$ m^2.

Mercury Intrusion Porosimetry (MIP) measurements have been performed by an external laboratory on the 2.5-cm length × 1.25-cm diameter samples to monitor any porosity alteration after CO_2 exposure. The measurements were performed on one or two cores, for sound samples and for samples exposed to CO_2. Before the measurements, all the samples were dried at 100°C during 60 hours. Pressure was applied to the mercury in progressive increments, and the corresponding intruded volumes were monitored. Two intrusion-extrusion cycles were performed to determine irreversible and reversible intrusion volumes. The maximum intrusion pressure was 70 MPa. Therefore, the results obtained represent the porosity filled with mercury at this pressure, *i.e.* the volume of pores connected to the surface through a percolative network, with a diameter greater than 18 nm. The precision of the measurements is around 1%.

In addition to the Mercury Intrusion Porosimetry, some water diffusion tests were performed on the 2.5-cm length × 1.25-cm diameter samples. The method consists of measuring the water loss during drying at 25°C under dried atmosphere. The weight loss represents the weight (or volume) of the evaporated water, some water remaining trapped by capillary forces. Considering the initial volume of sample, a plot of the variation of volume loss (%) *versus* square root of time is obtained. The initial slope gives information on the water diffusivity/permeability inside the rock and the value at the plateau corresponds to the sample porosity.

For mineral-phase identification through the samples, pieces (10 to 50 mg) were extracted from the edges and the centre of the samples. Then the sample pieces were ground for powder X-Ray Diffraction (XRD) analyses with a D5000 *Siemens* diffractometer.

Thin sections of the samples before and after exposure were also prepared for observations under optical microscope. The samples before and after exposure to CO_2 were cut to prepare polished sections in the longitudinal diameter plane of the core sample. Scanning Electron Microscope (SEM) observations were made on these sections in Secondary Electron (SE) or Back-Scattered Electron (BSE) modes to obtain information on their mineralogical changes. An *Hitachi* S-3400/N instrument at SRPC, coupled with an Electron Dispersive Spectrometer (EDS) device (Noran system Six model from *ThermoElectron corp.*) has been used. For the EDS analyses, the following elements were consistently measured: Mg, Al, Si, S, P, Ti, Na, Cl, K, Ca and Fe.

The Lavoux limestone samples were analyzed under Raman spectroscopy (*Renishaw Invia* microspectrometer; at the École Normale Supérieure, Paris) to investigate if some dissolution and new-precipitation processes may have formed other polymorphs of calcium carbonates than calcite (*i.e.* vaterite, aragonite).

Finally, in order to detect any porosity gradients along the samples, related to dissolution/precipitation processes, BSE

images obtained with the SEM were analyzed using an image processing software. The image was binarized by thresholding the grey-level scale to a value giving the best fit of the black parts of the initial image. The proportion of the black pixels of the binary image was measured and considered to correspond to a 2-D porosity [7, 22]. In order to check the repeatability of this method, at least three porosity measurements on the same selected zone were done to estimate the average and the standard deviation of the local porosity. Furthermore, two reference sandstones with porosity of 20% and 10% respectively, estimated by standard porosity methods, were used as standard rocks to control the efficiency of this method *(Fig. 2)*. The method gives good constraints for pore size greater than 1 μm. This pore scale differs from that of MIP measurements, which provides information on the pore-entrance size, down to 18 nm. Furthermore, the estimate is a two-dimensional porosity corresponding to a relative porosity. It is comparable between samples that underwent different durations of CO_2 exposure, but is not an absolute porosity value.

2 RESULTS FOR THE LAVOUX LIMESTONE

After the one-month exposure of the twenty samples at 28 MPa and 90°C in both CO_2 fluids, the limestone cores did not exhibit any visible alteration. They have kept their

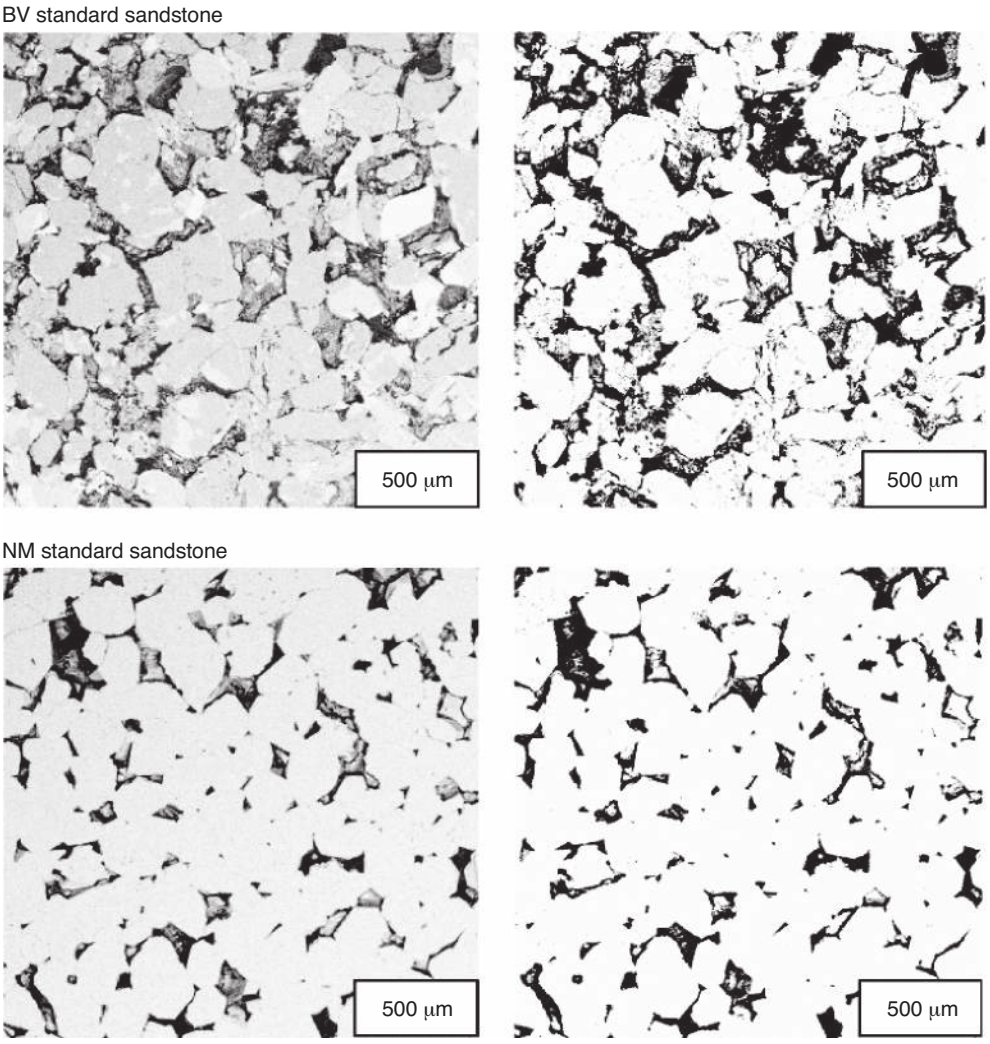

Figure 2

Binarization (right) of the initial grey-scale SEM-BSE images (left) of two sandstones using the threshold tool of an image processing software. The two sandstones ("BV" and "NM") images are standards for calibrating the BSE image analysis. The proportion of the black pixels of the binary images is considered to correspond to the two-dimensional porosity.

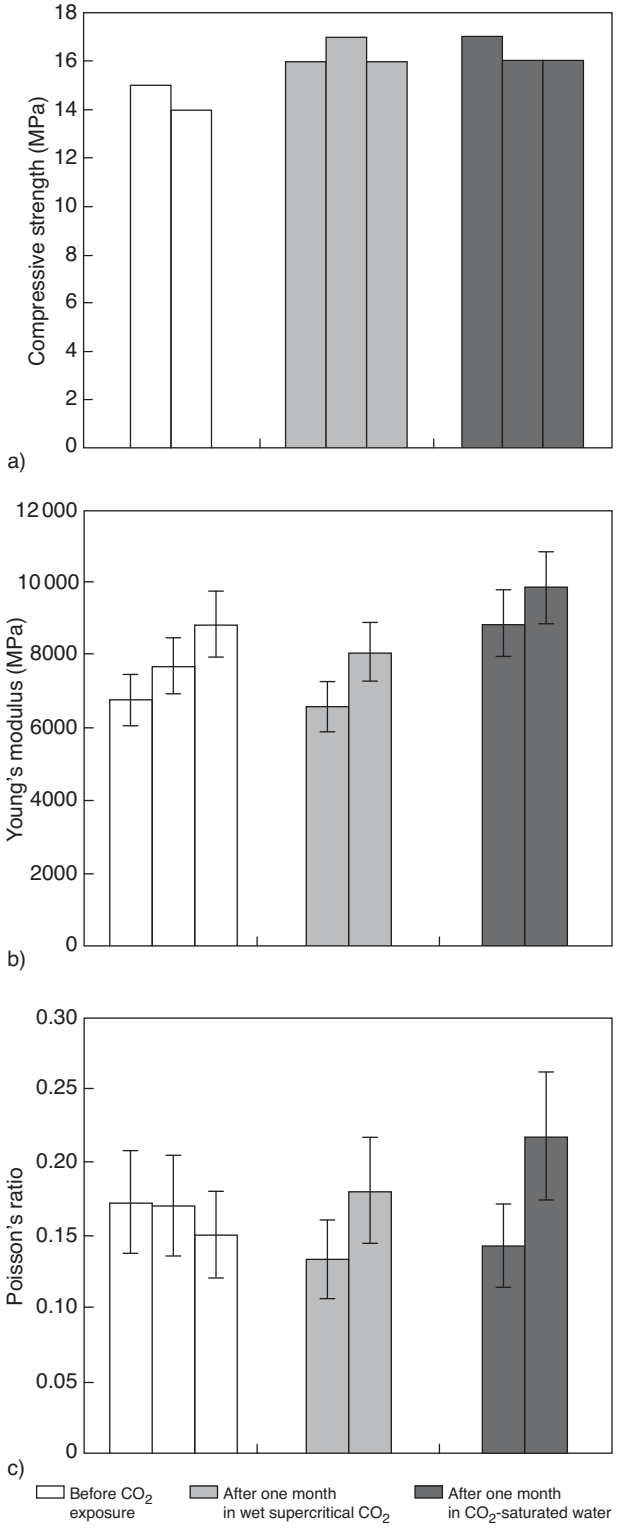

Figure 3

Evolution of the compressive strength a), the Young's modulus b) and the Poisson's ratio c) of the Lavoux limestone exposed to wet supercritical CO_2 and CO_2-saturated water during one month under reservoir conditions (28 MPa and 90°C). Each bar corresponds to a measurement done on one sample.

integrity. Neither dissolution features nor macroscopic crack occurrence were observed.

The dimensions of the samples (length and diameter) did not change after exposure to CO_2. However, their weight and specific gravity decreased from 1 to 3%. Before exposure, the pH of water in equilibrium with the limestone cores was close to 8 after few days of immersion. Then the cores were exposed to wet supercritical CO_2 and CO_2-saturated water during one month. At the end of the experiment, the pH of the fluid within the autoclave was close to 6 after cooling and depressurization. Then, after having immersed the attacked limestone samples in distilled water during few days, the new pH of water in equilibrium with all the attacked sample cores (alteration by wet supercritical CO_2 or CO_2-saturated water) was equal to the initial one, *i.e.* 8.

2.1 Mechanical and Permeability Data

The initial compressive strength of the Lavoux limestone is close to 15 MPa. After exposure to CO_2, it was of the same order (in the range 16-17 MPa), whatever the CO_2 fluid in which the sample cores were immersed *(Fig. 3)*. The Young's modulus of the samples before exposure is 8000 MPa and remained roughly close to this value after CO_2 exposure, accounting for the error bars. The initial Poisson's ratio (transverse contraction/axial elongation) is 0.17. After the CO_2 alteration, the results were dispersed between 0.12 and 0.21. Therefore, the mechanical properties do not seem to be affected by the CO_2 exposure.

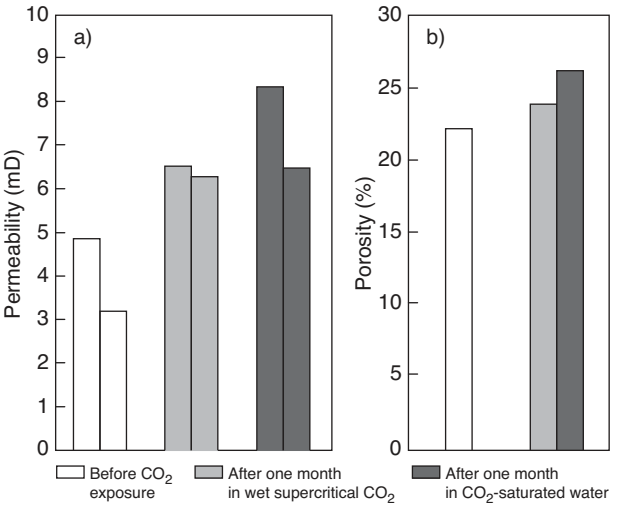

Figure 4

Evolution of the Lavoux limestone permeability deduced from water permeability measurements a) and porosity from Mercury Intrusion Porosimetry b) after exposure to wet supercritical CO_2 and CO_2-saturated water during one month under reservoir conditions.

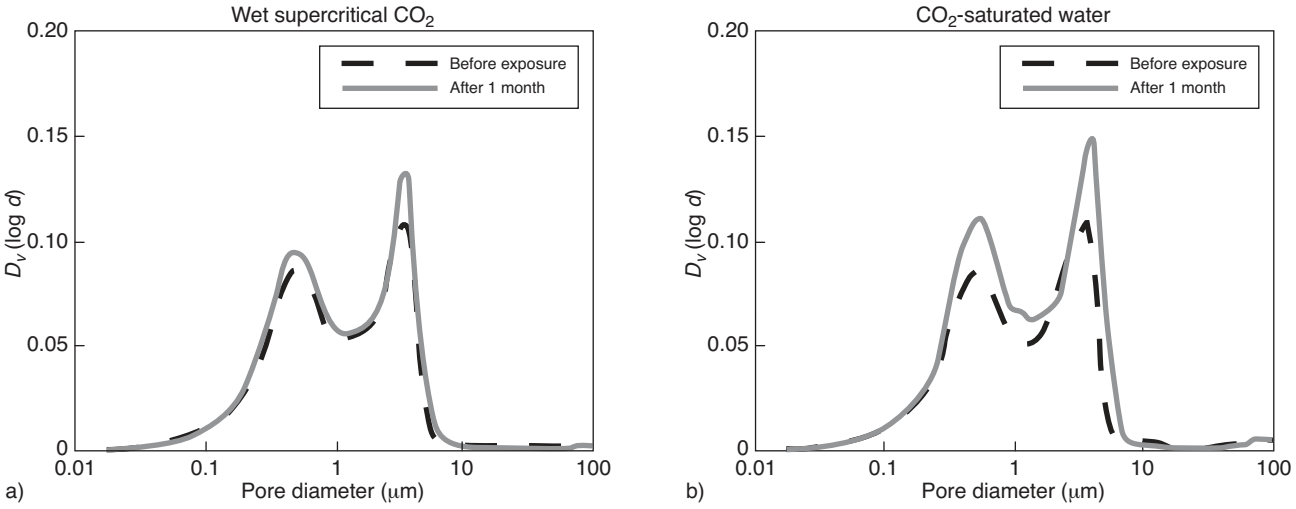

Figure 5

Evolution of the pore size distribution in the Lavoux limestone exposed to wet supercritical CO_2 and CO_2-saturated water during one month. For both cases, note the increase of the frequency of large pores.

Water permeability measurements on the Lavoux limestone cores show an initial permeability of 4 mD in average *(Fig. 4a)*. After exposure, the permeability was higher, with values between 6 and 6.5 mD for the samples exposed to wet supercritical CO_2, and between 6.5 and 8 mD for the samples immersed in CO_2-saturated water.

2.2 Porosity Data

MIP measurements show an initial porosity of 22% *(Fig. 4b)*. After one month, the porosity increase was 2% (Φ = 24%) in wet supercritical CO_2, and 4% (Φ = 26%) in CO_2-saturated water. The permeability increase previously highlighted was thus accompanied by an increase of porosity. The pore size distribution deduced from the MIP measurements showed a bimodal distribution with pore diameters of about 0.5 μm and 4 μm *(Fig. 5)*. Although the global porosity increased, the pore size distribution did not vary significantly after one-month exposure, whatever the CO_2 fluid. However, a slight increase of large pores frequency could be noted after alteration in both CO_2 fluids.

The water diffusion tests (water loss *versus* square-root of time) performed with the Lavoux limestone samples show a similar trend to that detected with MIP *(Fig. 6)*. The initial porosity, corresponding to the plateau on the graph, was about 20%. After exposure to wet supercritical CO_2, it increased to 23%. For the samples exposed to CO_2-saturated water, the porosity was about 26% after alteration. Both MIP method and water diffusion test show similar petrophysical evolution, indicated by an increase of the porosity after exposure. This increase was higher in CO_2-saturated water than in wet supercritical CO_2, but significant in both cases.

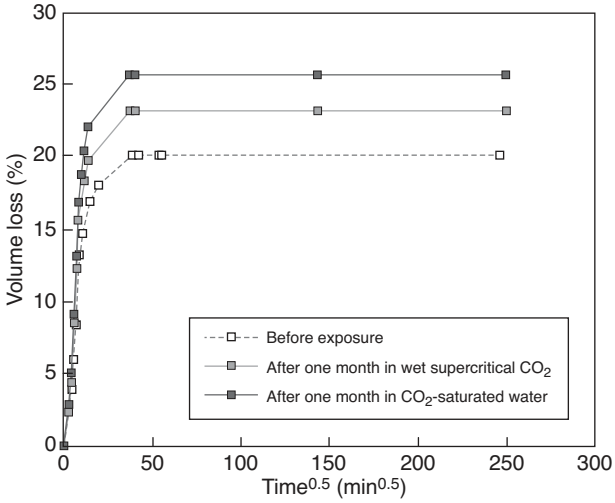

Figure 6

Evolution of the volume loss *versus* $\sqrt{(t)}$ obtained with the water diffusion tests for the Lavoux limestone before exposure and after one month in wet supercritical CO_2 and in CO_2-saturated water. The plateau corresponds to the porosity.

2.3 Mineralogy Data and Microstructure Observations

XRD spectroscopy analyses have been performed at the edges and in the middle part of the samples, before attack and after one-month exposure in both fluids. The Lavoux limestone contains nearly 100% calcite *(Fig. 7)*, without any

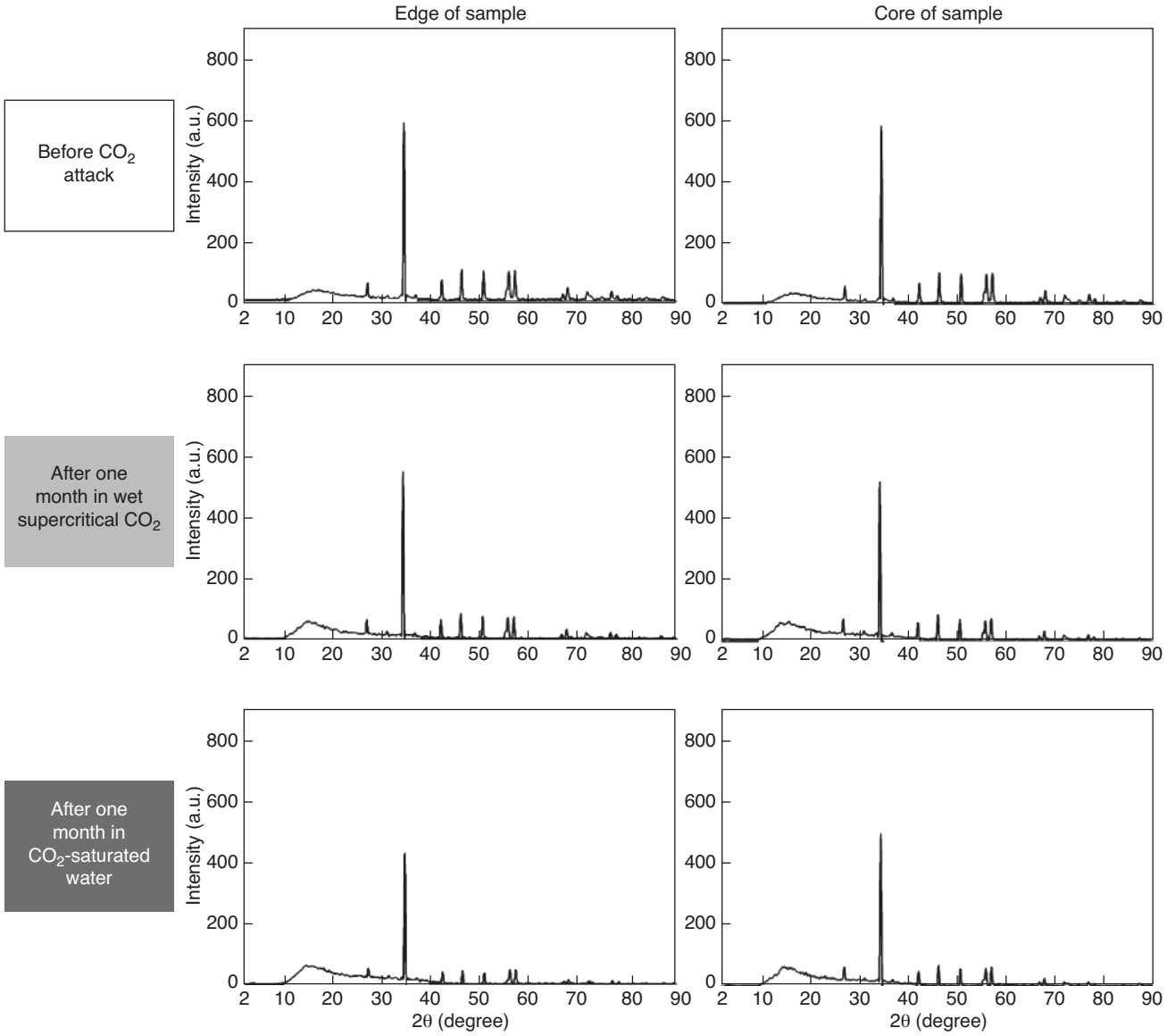

Figure 7

X-ray diffraction spectra showing the single occurrence of calcite in the samples of the Lavoux limestone (edge and middle part) before exposure and after one month of exposure to CO_2 fluids.

indication of neo-formed minerals that could have formed after exposure to CO_2 by dissolution/re-precipitation processes, such as other polymorphs of calcium carbonate, *i.e.* vaterite and aragonite. Raman spectroscopy analyses were performed through the samples, before and after exposure, in order to detect possible newly formed calcium carbonate polymorphs, even in very low amount and at the micrometer scale *(Fig. 8)*. This confirms XRD analyses: only calcite was present in the samples before and after the CO_2 exposure. Furthermore, the sample cross-sections of the Lavoux limestone samples exposed either to wet supercritical CO_2 or to CO_2-saturated water phase did not show a well-defined alteration front *(Fig. 8)*.

SEM was used to detect any dissolution pattern in the exposed samples compared to the initial limestone. Some microscopic dissolution features were deciphered, especially for the samples exposed to CO_2-saturated water during one month *(Fig. 9)*. Considering the pressure and temperature conditions of the test, and the high solubility of CO_2 since distilled water is used rather than brine, the pH of the fluid in the reactor during the test was low enough (pH ~ 3 under 28 MPa, 90°C; [21]) to destabilize calcite and initiate dissolution.

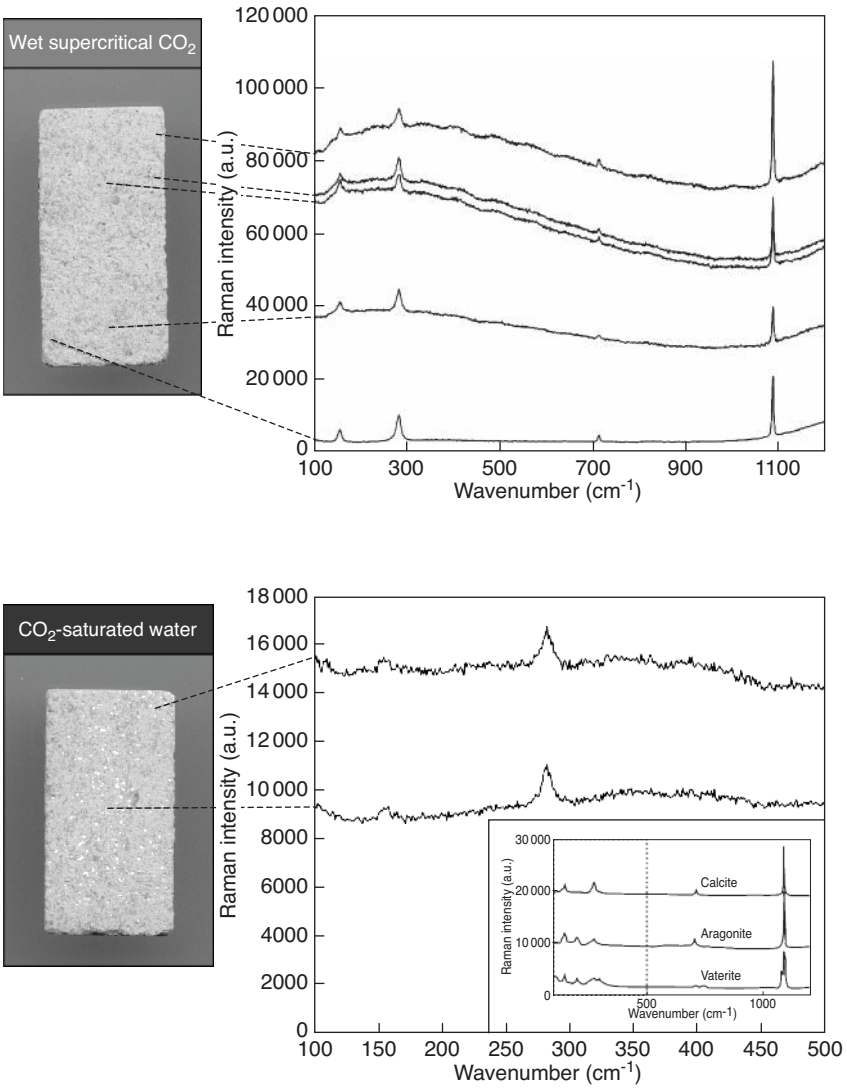

Figure 8

Raman spectra from the edge and the middle of the Lavoux limestone samples exposed to wet supercritical CO_2 (above) and to CO_2-saturated water (below) during one month. The Raman spectra for the three calcium carbonate polymorphs are shown in the lowermost part. The Raman intensity is given in arbitrary units (a.u.).

At a fixed pressure, the solubility of calcite decreases with an increase of temperature; in contrast, for a fixed temperature, the solubility of calcite in water increases with an increase of the pressure of CO_2 (*e.g.* [15]). Under the present test conditions (28 MPa, 90°C) when extrapolating the data of calcite solubility in water from [15], the solubility of calcite is quite high (*i.e.* $(1.5\text{-}2.0)\times10^{-2}$ mol $Ca^{2+}.kg^{-1}$ H_2O). This solubility value is about 6 times higher than the calcite solubility at the same temperature but under atmospheric pressure.

Local porosity estimates from SEM-BSE image analysis have been made through the Lavoux limestone samples, before and after CO_2 exposure. The initial local two-dimension porosity estimated in different areas of the polished sample cross-section is about 14±2% *(Fig. 10)*. After exposure to wet supercritical CO_2, the porosity profile shows local values ranging from 15 to 20%, accounting for the measurement uncertainties *(Fig. 11)*, higher than the initial porosity values. However, no clear porosity gradients could be identified across the sample, due to local porosity variations larger than the average porosity increase. Similarly to the Mercury Intrusion Porosimetry measurements, these profiles indicate global increase of the porosity due to the CO_2-exposure that is particularly significant for the samples exposed to CO_2-saturated water.

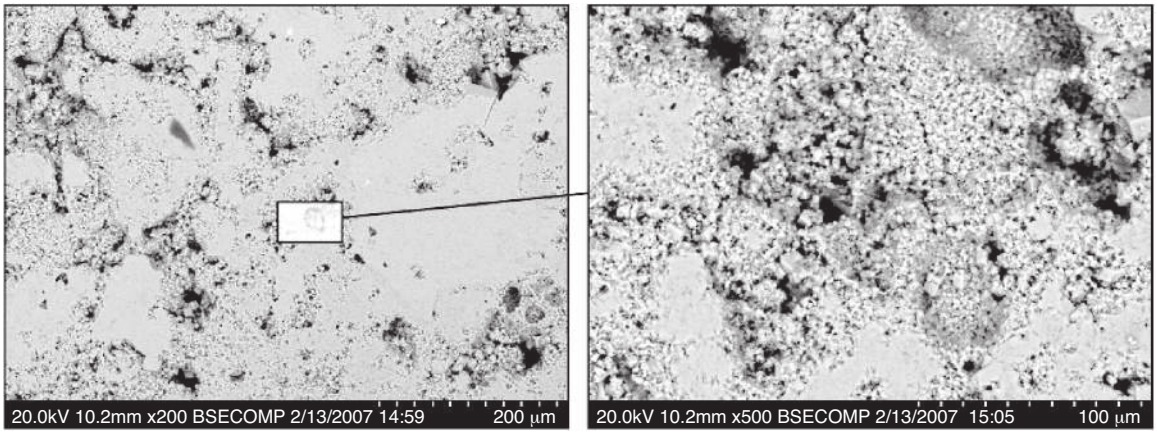

Figure 9

SEM-BSE images showing some microscopic dissolution structures within the samples of the Lavoux limestone exposed to CO_2-saturated water during one month.

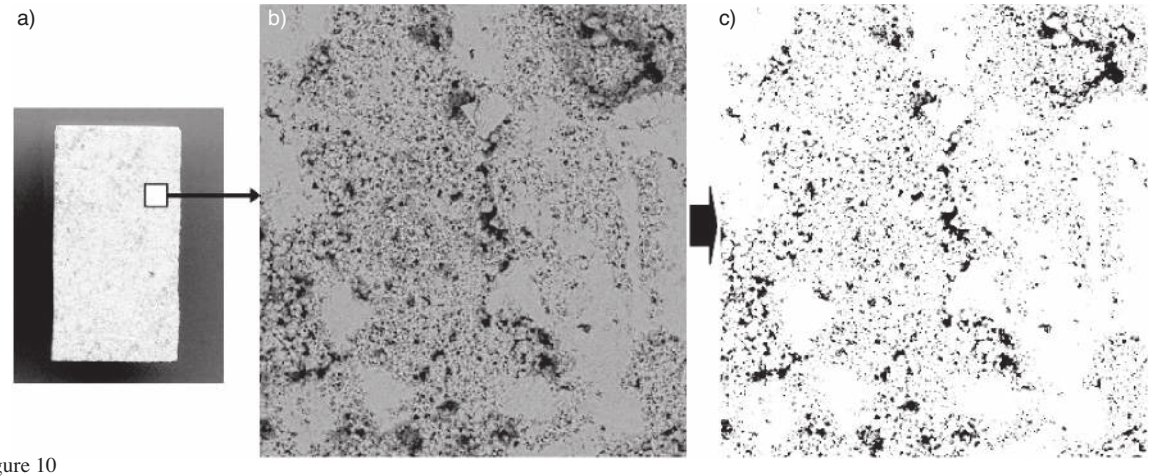

Figure 10

Sample cross-section a), grey-scale SEM-BSE images b) and binarized BSE image c) of the Lavoux limestone before CO_2 exposure. The proportion of the black part of the image corresponds to the local two-dimension porosity. Based upon estimates with a series of few binarized BSE images, the local porosity of the sound limestone is 14 ± 2%.

2.4 Interpretation

Therefore, after one month of CO_2 exposure at 28 MPa and 90°C, the limestone samples show a decrease of their weight and density, and an increase of their porosity (detected by MIP, water diffusion and SEM image analysis) and permeability. These observations may be attributed to microscopic dissolution of calcite during the CO_2 exposure. This increase is particularly well detected in the samples exposed to CO_2-saturated water, for which the transport of ionic species is enhanced compared to the wet supercritical CO_2 phase. However, no variation of the samples' mechanical properties could be deciphered. Such porosity increase has been observed after the one-month exposure; further tests at longer durations may be required to monitor the evolution of the limestone petrophysical properties over the long term to confirm this trend. Furthermore, it is noteworthy that this batch experiment has been done using distilled water rather than brine, the latter being subjected to a lower saturation of CO_2 [14] and thus to less severe conditions for the exposure of the samples. Any test using CO_2+formation water instead of CO_2+distilled water may be required to compare the evolution of the limestone petrophysical properties in CO_2-rich fluids under reservoir conditions. Indeed, the solubility of CO_2 depends on the ionic strength of the fluid. Furthermore cations and anions will act as a buffer and change the pH of the system. This will have an impact on the dissolution and/or precipitation of rock-forming minerals.

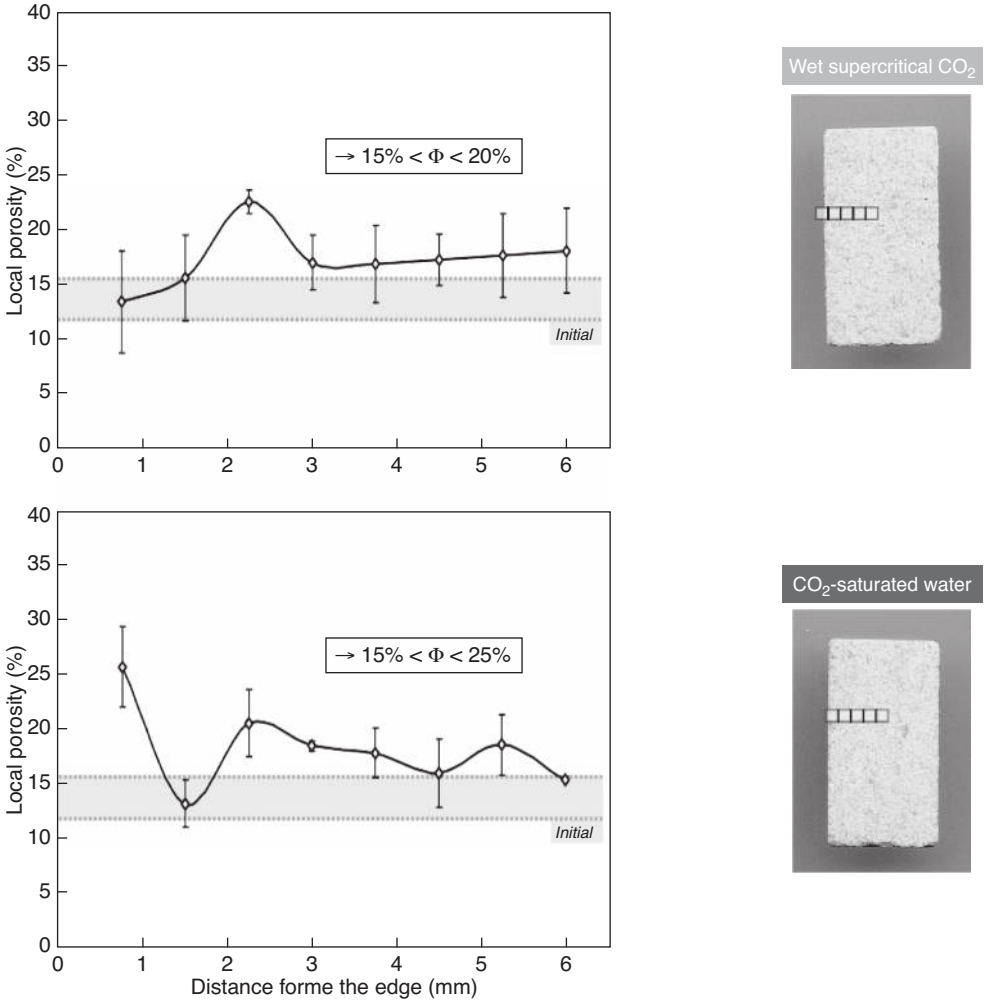

Figure 11

Cross-sections with localization of the areas chosen for SEM-BSE image analysis (left) and corresponding local porosity profiles (right) through the Lavoux limestone exposed to wet supercritical CO_2 (above) and to CO_2-saturated water (below). The grey area with dashed lines corresponds to the initial local porosity range (14±2%).

3 RESULTS FOR THE ADAMSWILLER SANDSTONE

After one month in the autoclave under 28 MPa and 90°C, the twenty cylindrical sandstone samples have preserved their initial aspect, whatever the fluid in which they were exposed. Their dimensions were identical as before exposure. In contrast to the limestone, the weight of the samples, as well as their specific gravity, showed a 3% increase after one month of exposure. Potential reasons could be a change in the clay mineral composition, sericitization of feldspars, or precipitation of carbonates.

Before exposure, the pH of water in equilibrium with the sandstones cores was close to 8 after few days of immersion. Then the sandstone cores were exposed to CO_2 during one month. At the end of the experiment, the pH of the CO_2-rich fluid within the autoclave was about 5 after cooling and depressurization. No change in the fluid color was observed before and after the one-month exposure. Then, after having immersed the sandstone samples in distilled water during few days, the new pH of water in equilibrium with the attacked sample cores was lower than the initial one (close to 7).

3.1 Mechanical and Permeability Data

The initial compressive strength of the Adamswiller sandstone was close to 25 MPa *(Fig. 12)*, above the initial strength of the limestone. After exposure to CO_2, the compressive strength data ranged between 19 and 27 MPa, around the

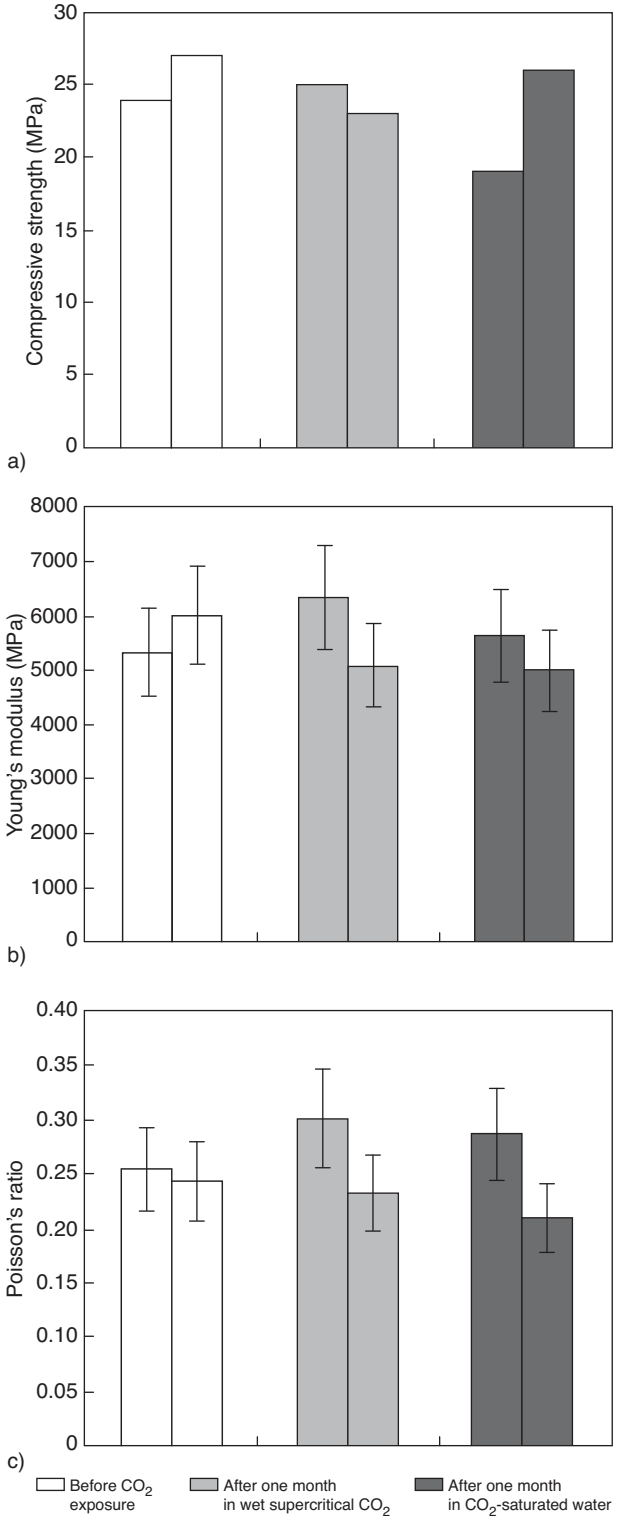

Figure 12

Evolution of the compressive strength a), the Young's modulus b) and the Poisson's ratio c) of the Adamswiller sandstone exposed to wet supercritical CO_2 and CO_2-saturated water during one month under reservoir conditions (28 MPa and 90°C). Each bar corresponds to a measurement done on one sample.

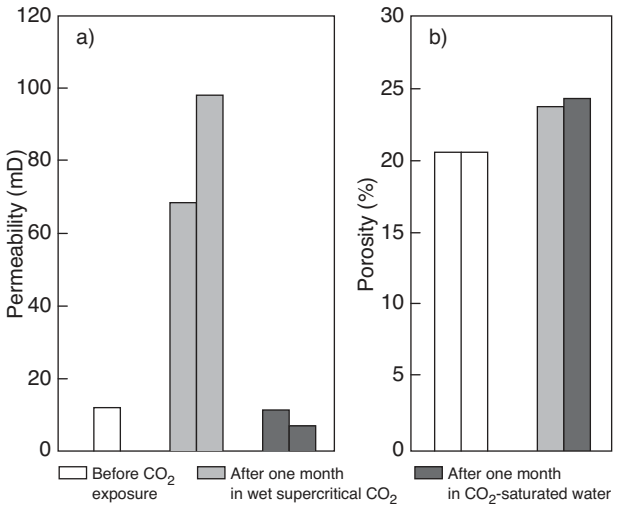

Figure 13

Evolution of the Adamswiller sandstone permeability deduced from water permeability measurements a) and porosity from Mercury Intrusion Porosimetry b) after exposure to wet supercritical CO_2 and CO_2-saturated water during one month under reservoir conditions.

values for the un-altered samples. The Young's modulus of the samples before exposure was 6000 MPa, and was roughly of the same value after exposure to either wet supercritical CO_2 or CO_2-saturated water *(Fig. 12)*. The mean Poisson's ratio was 0.25, before and after exposure to both CO_2 fluids *(Fig. 12)*.

The initial sandstone permeability was equal to 11 mD *(Fig. 13a)*. When exposed to wet supercritical CO_2, the permeability measurements show an increase of a factor 7 to 10 (permeability k = 70-100 mD). However, for the samples exposed to CO_2-saturated water, no change was detected *(Fig. 13a)*.

3.2 Porosity Data

The MIP measurements showed an initial porosity around 20% *(Fig. 13b)*. After one month, it increased of about 3% (Φ = 23.6%) in wet supercritical CO_2, and of about 4% (Φ = 24.2%) in CO_2-saturated water. The pore size distribution deduced from the MIP measurements showed a unimodal distribution with a pore diameter of about 10 μm *(Fig. 14)*. The pore size slightly increased to 20 μm after the one-month exposure in both CO_2 fluids.

The water diffusion tests (water loss *versus* square-root of time) performed with the Adamswiller sandstone samples show a similar trend *(Fig. 15)*. The initial porosity,

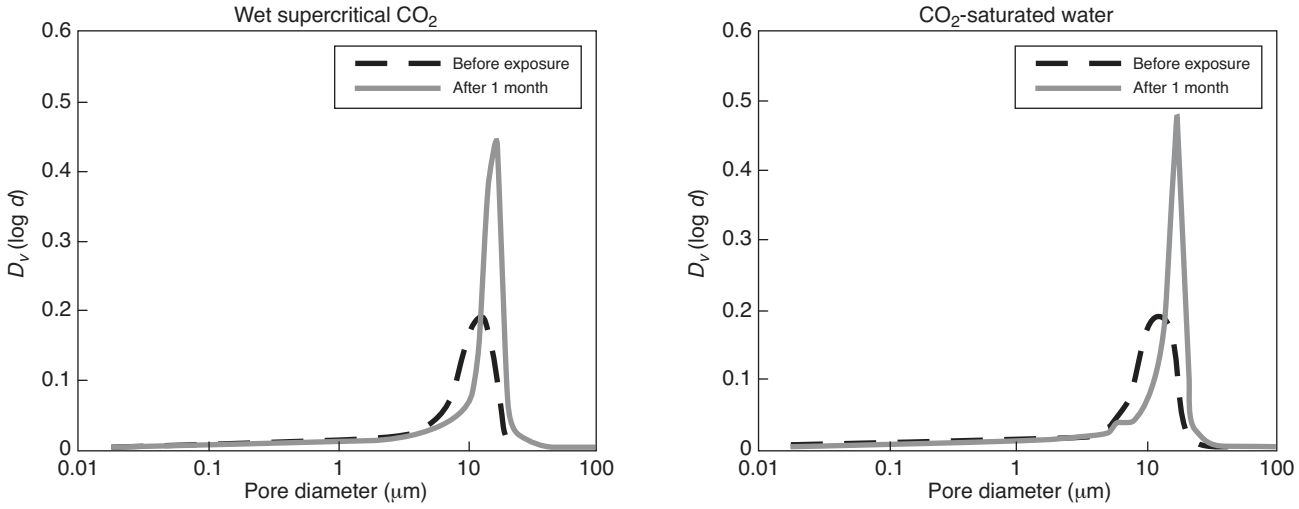

Figure 14

Evolution of the pore size distribution in the Adamswiller sandstone exposed to wet supercritical CO_2 and CO_2-saturated water during one month.

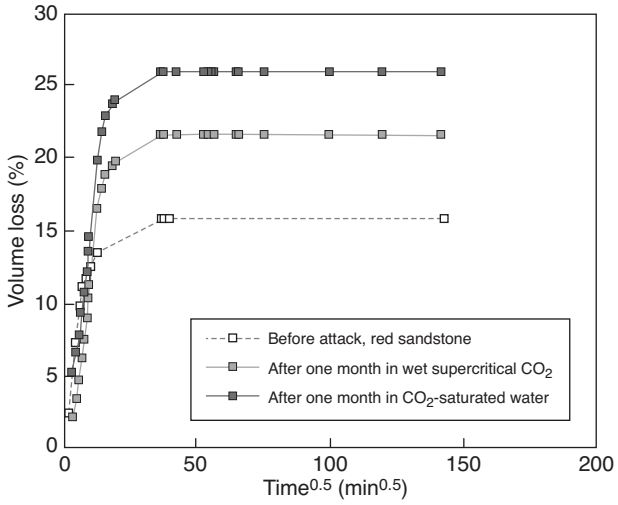

Figure 15

Evolution of the volume loss *versus* $\sqrt{(t)}$ obtained with the water diffusion tests for the Adamswiller sandstone before exposure and after one month in wet supercritical CO_2 and in CO_2-saturated water. The plateau corresponds to the porosity.

corresponding to the plateau on the graph, was about 16%. It has been measured in both the red and green parts of the sandstone. After exposure to wet supercritical CO_2, it increased to 22%. For the samples exposed to CO_2-saturated water, the plateau was at about 26%. As for the Lavoux limestone, the porosity increase was larger after exposure in CO_2-saturated water than in wet supercritical CO_2, and significant for both exposure conditions.

3.3 Mineralogy Data and Microstructure Observations

Similarly to the Lavoux limestone, the sample cross-sections of the Adamswiller sandstone exposed to wet supercritical CO_2 or CO_2-saturated water phase do not reveal any visible alteration front under SEM observation. Furthermore, when analyzing the mineral phases occurring at the edge and in the middle of the samples, before and after exposure, no difference can be deciphered from X-ray diffraction spectroscopy analyses. The samples were mainly made of K-feldspars and quartz, with low amounts of micas and chlorite.

Analyses under SEM were performed to investigate the microstructure of the sandstone before and after alteration and EDS analyses were systematically done. Figure 16 shows an example of the commonly encountered minerals in the Adamswiller sandstone. The only source of calcium encountered in the sandstone that could have reacted with CO_2 to form calcium carbonates is located in apatite, occurring in very low amount in the sandstone. Nevertheless, no trace of calcium carbonate could be found. Furthermore, no clear dissolution pattern was observed in the exposed samples. The increase of permeability and porosity shown previously may be related to a transformation of the clay minerals when reacting with CO_2 under low pH conditions [23], which was not clearly detectable under the microscope. Other minerals present in the sandstone should not react significantly over a one month period under our experimental conditions.

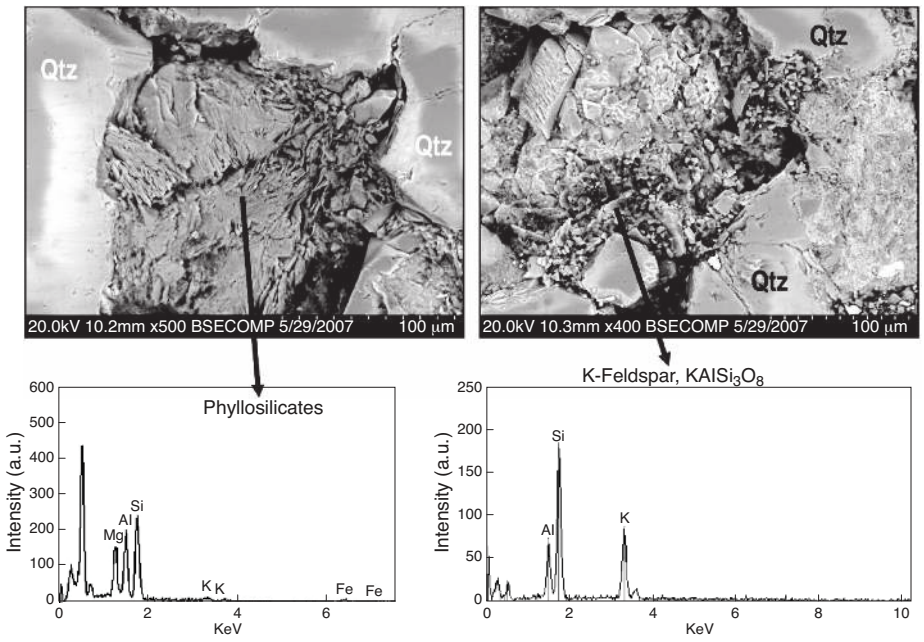

Figure 16

SEM-BSE images (above) and EDS analyses (below) of the Adamswiller sandstone after one month of CO_2 exposure to wet supercritical CO_2.

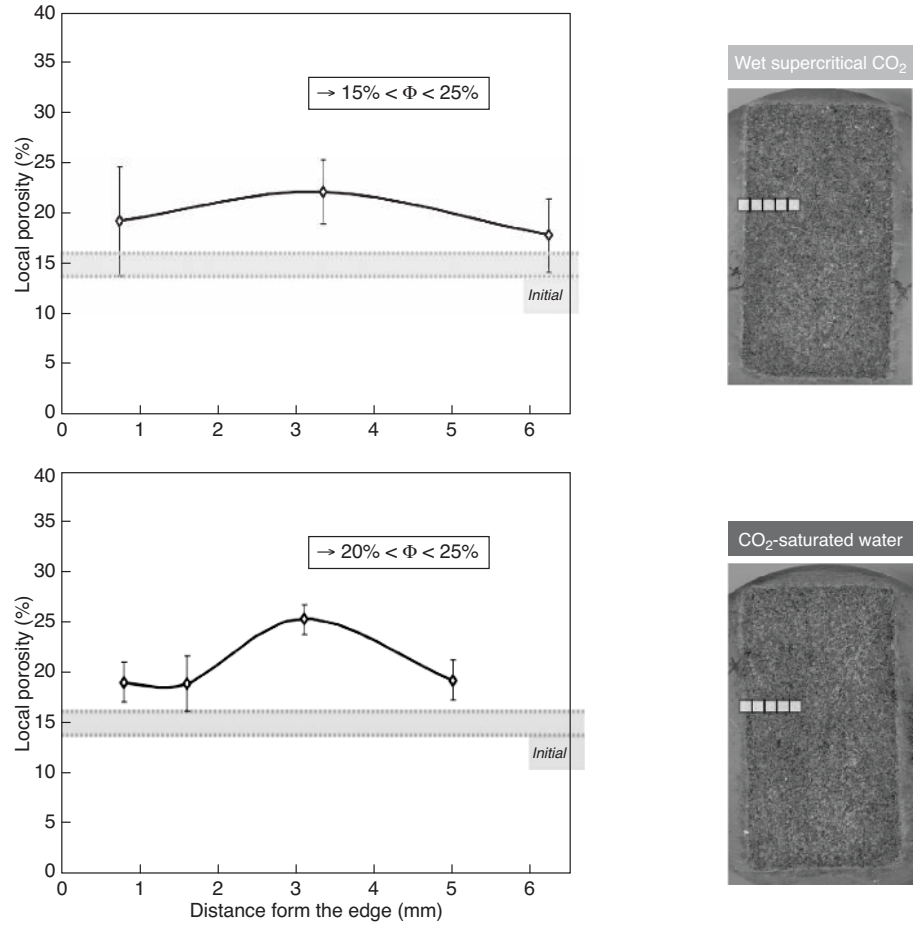

Figure 17

Cross-sections with localization of the areas chosen for SEM-BSE image analysis (left) and corresponding local porosity profiles (right) through the Adamswiller sandstone exposed to wet supercritical CO_2 (above) and to CO_2-saturated water (below). The grey area with dashed lines corresponds to the initial local porosity range (15±1%).

As for the Lavoux limestone, local porosity was estimated for the Adamswiller sandstone. The initial local porosity was equal to 15±1%. After one month in wet supercritical CO_2 and in CO_2-saturated water, the porosity profiles ranged between 15% and 25% and between 20% and 25% respectively, without drawing any clear pattern of porosity gradient *(Fig. 17)*. These profiles also highlight a slightly higher porosity increase in the CO_2-saturated water phase than in wet supercritical CO_2. This was also confirmed by water diffusion tests or Mercury Intrusion Porosimetry.

3.4 Interpretation

Therefore, as for the limestone, the sandstone samples exposed to CO_2 during one month under 28 MPa and 90°C did not show any change of their mechanical properties. However, a porosity increase, higher in CO_2-saturated water than in wet supercritical CO_2, has been detected either by MIP, water diffusion and SEM image analysis, and may be related to some clay mineral reorganization during the CO_2 exposure. The permeability increased significantly in the wet supercritical CO_2, whereas it remained equal to the initial value for the sample exposure to CO_2-saturated water, which is actually not clearly understood. One should note that these variations of the sandstone petrophysical properties were observed for single duration, and using distilled water. As commented for the Lavoux limestone, further tests performed at longer durations, using either distilled water or formation water, may be required to monitor the evolution of the sandstone in CO_2 environment under reservoir conditions.

CONCLUSIONS

A CO_2 equipment and procedure have been developed to simulate fluid - rock interactions under no-flow conditions, relevant for CO_2-storage at 3 km depth. Lavoux limestone and Adamswiller sandstone samples, exposed to CO_2 during one month, did not show any variation of mechanical properties. Their mineralogical characteristics were also preserved. However, the porosity of both rocks increased after CO_2 exposure, as attested either by MIP, water diffusion or SEM image analysis. For the limestone, this porosity increase was accompanied with a permeability increase. This alteration can be attributed to micro-dissolution of calcite, confirmed by SEM observations. This increase was well detected in the samples exposed to CO_2-saturated water, for which of the solubility of ionic species is higher in the liquid phase, compared to the wet supercritical CO_2 phase. However, for both fluid compositions (aqueous or supercritical CO_2), a significant porosity increase could be measured. For the sandstone, it was assumed that clay minerals may have reacted with CO_2 and controlled the porosity increase. This porosity increase was homogeneous through the samples, since no particular pattern of porosity gradient could be measured in the samples exposed to wet supercritical CO_2 and to CO_2-saturated water.

These observations bring new knowledge on the reservoir rocks reactivity under CO_2 conditions, even if our experimental conditions, especially the fluid composition, are far from those found in natural reservoirs. Our results show that, even when there is no fluid flow, both CO_2-wet and CO_2-saturated water may react with the rocks, although acknowledging that CO_2-saturated water is more reactive. Nevertheless, the solubility of CO_2 decreasing with the fluid salinity increase, the use of CO_2+distilled water rather than CO_2+brine allows providing an accelerating effect and appreciating the behavior of materials under acid environment during a relative short duration of exposure. The conditions of tests are thus rather severe for these rocks subjected to CO_2 fluids. Further tests using CO_2+formation water (brine) instead of CO_2+distilled water may be required to evaluate the evolution of the limestone and sandstone petrophysical properties under reservoir conditions. Furthermore, other tests at longer durations may also be needed to monitor the behavior of these rocks over the long term. Finally, it should also be emphasized that our experimental results do show that rocks are reactive in the presence of CO_2, even if they are only in contact with supercritical CO_2. This effect should be taken into account in the long-term simulations of a geological storage site.

ACKNOWLEDGEMENTS

The authors would like to thank the management of *Schlumberger* for permission to publish this paper. The laboratory staff of *Schlumberger* Riboud Product Center, especially Yamina Boubeguira and Hafida Achtal, is gratefully acknowledged. At the École Normale Supérieure, Olivier Beyssac is thanked for his advices in the Raman spectroscopy analyses and Roland Caron is also acknowledged for the preparation of sample cross-sections. Finally, the authors thank three anonymous referees for thorough reviews.

REFERENCES

1 Power M.T., Leicht M.A., Barnett K.L. (1989) Converting Wells in a Mature West Texas Field for CO_2 Injection, *SPE Paper* 20099.

2 Mizenko G.J. (1992) North Cross (Devonian) Unit CO_2 Flood: Status Report, *SPE/DOE Paper* 24210.

3 McDaniel Branting J.K., Whitman D.L. (1992) The feasibility of using CO_2 EOR Techniques in the powder river basin of Wyoming, *SPE Paper* 24337, Casper, Wyoming.

4 Barlet-Gouédard V., Rimmelé G., Goffé B., Porcherie O. (2006) Mitigation strategies for the risk of CO_2 migration through wellbores, *IADC/SPE* 98924, Miami, USA, February.

5 Barlet-Gouédard V., Rimmelé G., Goffé B., Porcherie O. (2007) Well Technologies for CO_2 Geological Storage: CO_2-resistant cement, *Oil Gas Sci. Technol.* **62**, 3, 1-12.

6 Barlet-Gouédard V., Rimmelé G., Porcherie O., Quisel N., Desroches J. (2008) A solution against well cement degradation under CO_2 geological storage environment, *Int. J. Greenhouse Gas Control* **3**, 206-216.

7 Rimmelé G., Barlet-Gouédard V., Porcherie O., Goffé B., Brunet F. (2008) Heterogeneous porosity distribution in Portland cement exposed to CO_2-rich fluids, *Cement Concrete Res.* **38**, 1038-1048.

8 Kutchko B., Strazisar B., Dzombak D., Lowry G., Thaulow N. (2007) Degradation of well cement by CO_2 under geologic sequestration conditions, *Environ. Sci. Technol.* **41**, 4787-4792.

9 Jacquemet N., Pironon J., Caroli E. (2005) A new experimental procedure for simulation of H_2S + CO_2 geological storage - Application to well cement aging, *Oil Gas Sci. Technol.* **60**, 1, 93-206.

10 Carey J.W., Wigand M., Chipera S. *et al.* (2007) Analysis and performance of oil well cement with 30 years of CO_2 exposure from the SACROC unit, West Texas, USA, *Int. J. Greenhouse Gas Control* **1**, 75-85. doi:10.1016/S1750-5836(06)00004-1.

11 Bachu S. (2000) Sequestration of CO_2 in geological media: criteria and approach for site selection in response to climate change, *Energ. Convers. Manage.* **41**, 9, 953-970.

12 Wong T.F., David C., Zhu W. (1997) The transition from brittle faulting to cataclastic flow in porous sandstones: Mechanical deformation, *J. Geophys. Res.* **102**, 3009-3025.

13 Spycher N., Pruess K., Ennis-King J. (2003) CO_2-H_2O mixtures in the geological sequestration of CO_2. I. Assessment and calculation of mutual solubilities from 12 to 100°C and up to 600 bar, *Geochim. Cosmochim. Ac.* **67**, 16, 3015-3031.

14 Spycher N., Pruess K. (2005) CO_2-H_2O mixtures in the geological sequestration of CO_2. II. Partitioning in chloride brines at 12-100°C and up to 600 bar, *Geochim. Cosmochim. Ac.* **69**, 13, 3309-3320.

15 Portier S. (2005) Solubilité de CO_2 dans les saumures des basins sédimentaires. Application au stockage de CO_2 (gaz à effet de serre), *PhD Thesis*, Université Louis Pasteur, Strasbourg I.

16 Portier S., Rochelle C. (2005) Modelling CO_2 solubility in pure water and NaCl-type waters from 0 to 300°C and from 1 to 300 bar. Application to the Utsira Formation at Sleipner, *Chem. Geol.* **217**, 187-199.

17 Hollister L.S. (1981) *Information intrinsically available from fluid inclusions, in Fluid inclusions: applications to petrology*, Hollister and Crawford (ed.), *Mineral association of Canada*, Short course handbook, **6**, 1-12.

18 Blencoe J.G., Naney M.T., Anovitz L.M. (2001) The CO_2-H_2O system: III. A new experimental method for determining liquid-vapor equilibria at high subcritical temperatures, *Am. Mineral.* **86**, 1000-1111.

19 Blencoe J.G. (2004) The CO_2-H_2O system: IV. Empirical, isothermal equations for representing vapor-liquid equilibria at 110-350°C, $P \leq 150$ MPa, *Am. Mineral.* **89**, 1447-1455.

20 Schaef H.T, McGrail B.P. (2004) *Direct measurements of pH and dissolved CO_2 in H_2O-CO_2 brine mixtures to supercritical conditions*, Pacific Northwest National Laboratory, Richland, USA.

21 Toews K.L., Shroll R.M., Wai C.M. (1995) pH-defining equilibrium between water and supercritical CO_2. Influence on SFE of organics and metal chelates, *Anal. Chem.* **67**, 4040-4043.

22 Tovey N.K., Hounslow M.W. (1995) Quantitative micro-porosity and orientation analysis in soils and sediments, *J. Geol. Soc. London* **152**, 119-129.

23 Abdullah W.S., Alshibli K.A., Al-Zou'bi M.S. (1999) Influence of pore water chemistry on the swelling behavior of compacted clays, *Appl. Clay Sci.* **15**, 447-462.

Final manuscript received in September 2009
Published online in November 2009